Numerical investigations of repairable dissipative bolted fuses for earthquake resistant composite steel frames

Marco Valente *, Carlo A. Castiglioni, Alper Kanyilmaz

Department of Architecture, Built Environment & Construction Engineering ABC, Politecnico di Milano, Piazza Leonardo da Vinci 32, 20133 Milan, Italy

This study presents the main results of the numerical investigations carried out on an innovative repair-able fuse device for dissipative beam-to-column connections in moment-resisting composite steel frames. The fuse consists of steel plates bolted to the web and bottom flange of the beam with a specif-ically detailed gap in the concrete slab. The behavior of the fuse device is studied by means of two dif-ferent numerical approaches. Numerical analyses performed on detailed three-dimensional finite element models of beam-to-column sub-assemblages show that potential damage concentrates only in the fuse section, without any significant damage in the other structural elements. Repair work, if needed, is therefore limited to the replacement of the fuses only. The effects of some geometrical characteristics of the flange plates on the behavior of the fuses are investigated. In order to extend the results of the numerical analyses to multi-storey frames subjected to seismic excitations, simple numerical models of the device are developed and calibrated through the experimental results of laboratory tests. Non-linear dynamic and static analyses are performed on multi-storey composite steel frames and the effec-tiveness of the fuse devices is evaluated. The influence of the main mechanical characteristics of the dif-ferent devices on the seismic performance of several composite steel frames is also discussed for various ground motion intensity levels. Experimental and numerical results show that it is possible to success-fully dissipate energy and concentrate plasticity by means of the fuse system, along with simple and cost effective repairability.

Keywords:
Dissipative bolted fuse device
Beam-to-column connection
Numerical model
Steel frame
Energy dissipation
Non-linear dynamic analysis

1. Introduction

Modern seismic codes allow for significant plastic deformations in dissipative zones of building structures under design seismic actions, provided that the integrity of both individual members and the structure as a whole is not endangered. The design seismic loads are considerably reduced, as compared to elastic design, for building structures designed for energy dissipation and ductility. This design philosophy results in increasing concerns with the repairability of structures damaged by severe earthquakes.

As regards steel buildings, the large number of beam-to-column connection failures observed in moment-resisting frames in past earthquakes caused very high repair costs. New design approaches have been proposed for moment-resisting frame connections, implementing solutions that aim at shifting the plastic hinge and the associated large plastic deformations into the beams, away from the potentially brittle beam-to-column connection welds. The reduced beam section (RBS) connection [1] is an option for improving the ductility of steel beam-to-column connections in high seismicity regions. This solution has been extensively studied and is able to concentrate plasticity and provide energy dissipation, as shown, among the others, in [2]: nevertheless, the repair of the beam damaged by severe earthquakes presents serious practical difficulties. Simple and cost-effective repairability of the damaged parts of the beam represents a crucial issue and a challenging research item. Therefore, new design approaches are intended to develop devices that can simultaneously dissipate energy through the non-linear behavior of their components and be easily repaired.

The majority of past experimental and numerical research on dissipative and easy-replaceable fuses has been devoted mainly to steel braced frame structures and significant developments have been achieved. Dubina et al. [3] investigated eccentrically braced frames with removable links connected to the beams using flush end-plate bolted connections. High-strength steel was used for members outside links in order to enhance the global seismic performance of the structure by constraining plastic deformations to removable links and reducing permanent drifts of the structure. Mansour et al. [4] presented an experimental research program

Article history:
Received 29 March 2016
Revised 28 October 2016
Accepted 3 November 2016
Available online 15 November 2016

* Corresponding author.
E-mail address: marco.valente@polimi.it (M. Valente).

Published Journal Article available at: http://dx.doi.org/10.1016/j.engstruct.2016.11.004

to develop and assess the design of replaceable links for eccentric braced frames. The test program included cyclic tests on both individual link specimens and full-scale eccentrically braced frame sub-assemblages. Tan and Christopoulos [5] presented the development of replaceable cast steel links for eccentric braced frames that integrate the advantages of replaceable yielding links with the benefits of steel castings to achieve large ductility. Two types of replaceable link configurations with alternate link-to-beam connections were tested. Plumier et al. [6] developed innovative dissipative systems for concentric braced frames, comprising pinned and "U" type connections: the application of such innovative systems to concentric bracings in steel frames and to other types of structures is shown in [7,8]. Chan et al. [9] conducted an experimental study on a metallic passive energy dissipative device that utilizes plastic shear deformation of diaphragm steel plate. Giannuzzi et al. [10] proposed an innovative seismic-resistant steel framing system capable of providing stiffness and ductility to new or existing structures. The bracing system consists of concentric X-braces connected in series with rectangular sacrificial shear panels. The braces are designed to remain elastic during seismic events, while the shear panels are sized and configured to dissipate energy through stable hysteretic behavior.

Focusing on moment resisting frames, Koetaka et al. [11] presented a novel beam-to-column moment connection suitable for the column weak axis: a wide-flange beam was joined to a wide-flange column by bolted splices at the top flange and hysteretic dampers at the bottom flange. Oh et al. [12] developed a repairable beam-to-column connection system with a slit damper connected to the bottom flange of the beam using high-strength bolts. Balut and Gioncu [13] suggested two replaceable "dog-bone" solutions for moment-resisting frames: the dissipative element could be an I-beam with end plates or two channels bolted to the beam. Shen et al. [14] conducted combined analytical and large-scale experimental studies to validate two types of replaceable link with different bolted connections. Vargas and Bruneau [15] investigated a design approach to concentrate damage on removable structural elements, with the main structure designed to remain elastic or with minor inelastic deformations.

This study is part of the "Fuseis" project that aims at developing innovative types of seismic-resistant composite steel frames with dissipative fuses. The devices are made by introducing a discontinuity in the composite beams of a moment-resisting frame and assembling the two parts of the beam through steel plates bolted or welded to the web and flange of the beam. Within the "Fuseis" project, experimental tests on beam-to-column specimens and frame sub-assemblages equipped with fuse systems were carried out at Instituto Superior Tècnico (IST) of Lisbon and at Politecnico di Milano: bolted and welded fuse device solutions were experimentally tested and the main results are reported in [16–19].

The work described in this paper presents the main results of the numerical investigations conducted on the bolted fuse devices shown in Fig. 1. The behavior of the bolted fuse devices and the effects on the seismic performance of composite steel frames are analyzed through two different numerical approaches. First, the refined finite element modeling technique, for which the computational effort is very heavy, is used to develop detailed three-dimensional finite element (FE) models of beam-to-column sub-assemblages with fuse devices by means of the computer code ABAQUS [20]. Numerical analyses are conducted in order to have a better understanding of the response of the connections equipped with the device and to demonstrate that the whole plasticization occurs in the fuses only. The effects of different geometric properties of the flange plate, such as thickness, cross section area and free buckling length, on the response of the fuse are also investigated and comparisons with the results of the experimental tests are made. Moreover, the refined three-dimensional FE models are used to obtain some mechanical characteristics (elastic stiffness and moment resistance capacity under sagging and hogging rotations) of fuses that were not tested during the experimental campaign.

Then, simple numerical models are developed by means of the commercial software SAP2000 [21] in order to investigate the seismic response of multi-storey composite steel frames. After the calibration of the numerical models according to the results of experimental tests, non-linear dynamic and static analyses are carried out on different types of steel frames with fuse devices, in order to simulate more realistic cases and evaluate both the response of the fuses and the global behavior of the structures. The seismic performance of multi-storey frames with and without fuse devices is compared for various ground motion intensity levels in terms of top displacement, base shear, plastic energy dissipation, residual drift and damage distribution.

2. Experimental tests

Within the "Fuseis" research project, two types of experimental tests were carried out in order to assess the performance of the fuse devices under cyclic actions. The laboratory tests performed at Instituto Superior Tècnico of Lisbon were aimed at characterizing the behavior of the device in terms of moment-rotation curves. Then, a portion of a full-scale composite steel frame with fuse devices was tested at Politecnico di Milano in order to simulate a real scale case.

2.1. Laboratory tests at Instituto Superior Tècnico of Lisbon

The experimental test set-up and the beam-to-column sub-assemblage with the fuse device configuration used in the laboratory tests at Instituto Superior Tècnico of Lisbon are shown in Fig. 2. To assess the performance of the fuse device, experimental tests were conducted on different sub-assemblages of beam-to-column joints, imposing cyclic displacements at the free edge of the beam by means of an actuator. The proposed devices proved to be very easy to replace and were able to both concentrate plastic deformations in the steel plates and dissipate large amounts of energy through stable cyclic behavior. A detailed description of the specimens and the results of the extensive experimental campaign carried out at Instituto Superior Tècnico of Lisbon can be found in [17]. The longitudinal reinforcement of the 150 mm thick concrete slab consisted of ϕ20/100, top layer, and ϕ16/100 + ϕ 12/200, bottom layer (dimensions in mm). Full shear connection was provided between the slab and the steel beam by means of IPE100 sections (spacing = 150 mm) welded on the top of the beam flange, acting as shear studs. A pair of reinforcing plates ($230 \times 300 \times 6$ mm) were welded to the beam web near the fuse device and a pair of transverse beams (HEB200 profile) were placed in the column web at the beam-to-column joint. High strength friction grip (HSFG) bolts (size M16, class 8.8) were used to connect the steel plates to the beam in the fuse region. The bolts were tightened according to provisions given in EN 14399 [30] (minimum preload equal to 88 kN and coefficient of friction between the different surfaces equal to 0.2).

2.2. Laboratory tests at Politecnico di Milano

The experimental test set-up represents a portion of a storey of a composite steel frame, as shown in Fig. 3. The bases of the columns were restrained against horizontal and vertical displacements through pin connections and cyclic displacements were imposed at the top of the columns by means of an actuator. Full shear connection was provided between the slab and the steel

Fig. 1. Schematic drawing and general view of a beam-to-column joint with bolted fuse device used in the experimental tests carried out at Politecnico di Milano.

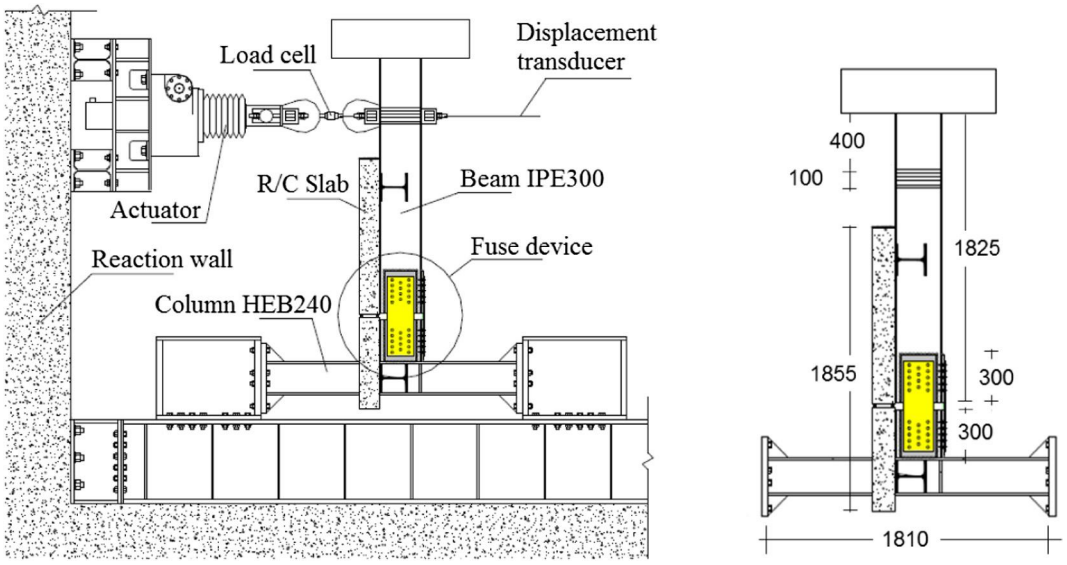

Fig. 2. Experimental test set-up and beam-to-column sub-assemblage.

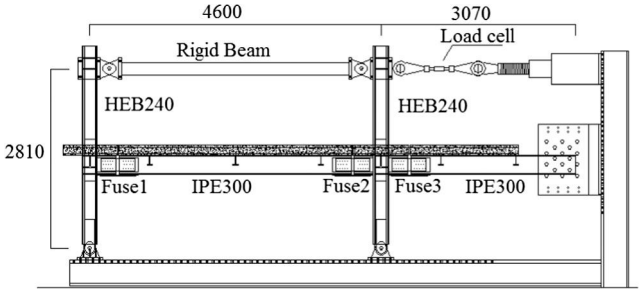

Fig. 3. Experimental test set-up, frame sub-assemblage and fuse device configuration.

beam. The beam-to-column connections were shop-welded and could be considered as rigid connections. The fuse devices were obtained by means of plates bolted to the web and the lower flange of the beam. The part of the beam near the connection was reinforced with steel plates welded to the web and to the flange. The same geometrical and mechanical characteristics of the beam-to-column specimens tested at Instituto Superior Tècnico of Lisbon were adopted for the frame sub-assemblage. Cyclic tests were performed on the frame sub-assemblage with four different fuses characterized by the same web plates and different flange plates. A comprehensive description of the specimens and the results of the experimental campaign on dissipative bolted fuses carried out at Politecnico di Milano are presented in detail in [16].

3. Numerical investigations through detailed FE models

Before the execution of the experimental tests, preliminary numerical investigations were carried out in order to evaluate the importance of the main design parameters (material properties and geometric dimensions) characterizing the fuse devices and to anticipate the overall behavior of the test specimens. Detailed three-dimensional finite element models can provide useful information about stress concentrations and plastic strain distributions [10,22,23]. Modifications concerning the members, connections and device properties (geometric and material) were made to achieve a satisfactory performance of the beam-to-column sub-assemblages. Preliminary numerical investigations led to the definition of optimal configurations for the bolted fuse devices.

3.1. Finite element models

Detailed three-dimensional finite element models of beam-to-column sub-assemblages with fuse devices were developed by using the ABAQUS software package [20] in order to reproduce the behavior of the fuse system under both monotonic and cyclic

loading, and to perform parametric analyses. Finite element models of a composite beam connected to a column were first created to identify the mechanical and geometrical parameters influencing the cyclic performance of the fuse device, Fig. 4. The devices were designed to be weaker than the adjacent members in order to concentate plastic deformations within the fuse, thus avoiding the spreading of damage in the irreplaceable non-dissipative zones. The cyclic behavior of the fuse was investigated changing selected geometric and mechanical parameters, such as the geometric slenderness and the resistance capacity ratio.

The geometric slenderness λ of the flange plate is defined as:

$$\lambda = \frac{L_0}{t_{fuse}} \tag{1}$$

where L_0 is the free buckling length of the fuse and t_{fuse} is the thickness of the fuse flange plate. The free buckling length L_0 is given by the horizontal distance between the innermost bolt rows of the fuses, as shown schematically in Fig. 4. Within this length both flange and web plates are unrestrained and therefore are free to buckle.

The resistance capacity ratio α of the fuse is defined as:

$$\alpha = \frac{M_{\max,fuse}}{M_{pl,beam}} \tag{2}$$

where $M_{max,fuse}$ is the maximum moment capacity developed by the fuse device and $M_{pl,beam}$ is the plastic resistant moment of the unreinforced area (away from the fuse, without the web and flange reinforcing plates) of the composite cross-section of the beam. The maximum moment of the fuse $M_{max,fuse}$ was computed with a design model described in [17]. The model takes into account the hardening and buckling phenomena and was validated through comparisons with the experimental tests. The plastic resistant moments of the composite cross-section were computed in accordance with the assumptions described in EN 1994 [26] for both sagging and hogging directions.

Then, the finite element models of beam-to-column sub-assemblages with composite slabs were used to reproduce the behavior of the specimens tested at Instituto Superior Tècnico of Lisbon, Fig. 5. The test specimen consisted of a typical beam-to-column sub-assemblage, comprising a composite beam with an IPE300 profile supporting a 150 mm thick and 1450 mm wide reinforced concrete slab and a HEB240 column. The column of the model was fixed at the edges simulating the boundary conditions of the experimental tests. All the dimensions and geometrical details of the FE model are the same as the specimens tested at Instituto Superior Tècnico of Lisbon and are reported in [17]. The fuse device was represented by steel plates bolted to the web and bottom flange of the beam with M16 bolts, along with a specifically detailed slab gap. The gap in the slab was intended to avoid damage to the concrete, allowing for large plastic rotations in the fuse. Longitudinal steel rebars were continuous over the gap and were designed by forcing the plastic neutral axis to lie within the slab thickness.

The details of the different flange plates with indications of all the dimensions are shown in Fig. 5 and the main geometric properties are summarized in Table 1.

Finally, a finite element model of a portion of a storey of a composite steel frame was developed in order to calibrate and reproduce the experimental tests performed at Politecnico di Milano, Fig. 6. The frame sub-assemblage consisted of two HEB240 steel columns, two IPE300 steel beams and a 150 mm thick reinforced concrete slab.

The elements used for the development of the models are solid (continuum) elements named C3D8R, which are linear displacement interpolation solid elements with reduced integration. Reduced integration elements are chosen in order to reduce computational time, which would be excessive in case of higher order elements. At least two elements are employed in the thickness of steel flanges, plates and stiffeners to accurately reproduce the bending behavior. The mesh is finer in the parts of the model where high stress concentrations are expected. The fuse device is modeled by introducing contact interactions among the beam, bolts and steel plates. Shear connection between slab and beam and all other constraints are modeled by using the "tie" option. Using this constraint type, the degrees of freedom (rotational and translational) between the nodes of the two surfaces which are "tied" to each other are constrained to maintain the same values.

Contact interactions are introduced to model the connection among the steel plates and bolts. Two surfaces should be defined in ABAQUS as contacting surfaces; one is the "master" and the other the "slave" surface. Contact among the different parts is defined as normal and tangential to the surfaces. The first type uses an augmented Lagrangian method to solve the equations and the second type models the friction between the two surfaces using

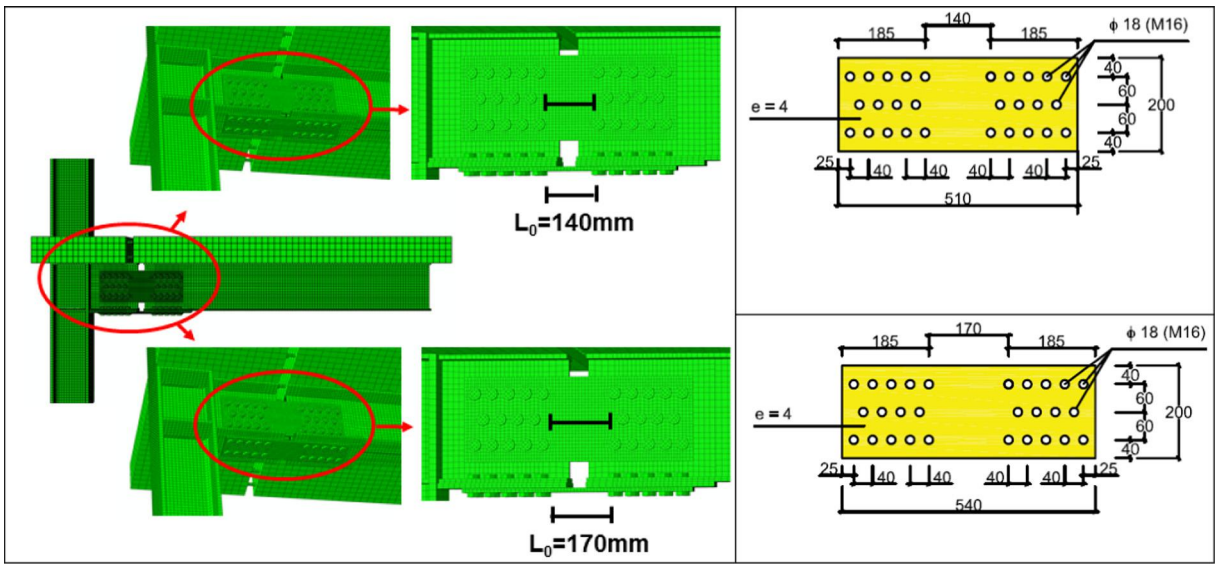

Fig. 4. FE model of a beam-to-column joint with different free buckling length L_0. Details and main dimensions (in mm) of the web plates.

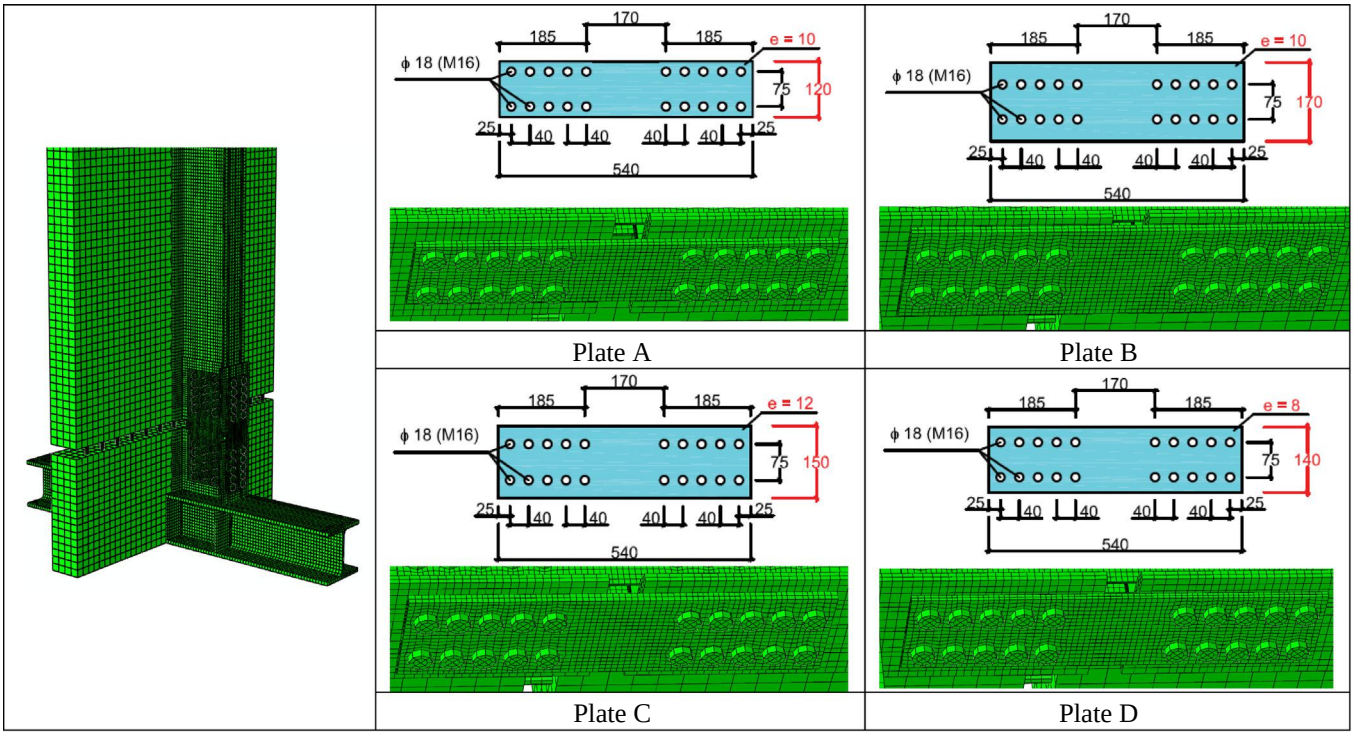

Fig. 5. FE model of a specimen used for the experimental tests and details of the different flange plates with indications of the main dimensions (in mm). Displacements are imposed at the free edge of the beam. Fixed restraints are applied at the two edges of the column.

Table 1
Summary of the main dimensions and geometric slenderness λ of the bolted flange plates of the different fuses (L_0 = 170 mm).

Flange plate	A	B	C	D
Thickness [mm]	10	10	12	8
Width [mm]	120	170	150	140
Cross-section area [mm^2]	1200	1700	1800	1120
Geometric slenderness λ	17	17	14.2	21.3

a penalty method and a friction coefficient defined by the user; the value given for this coefficient is 0.2. The bolt preload is simulated using the bolt load method in ABAQUS. Bolts are located centrally into the holes with a uniform clearance of 2 mm.

Structural steel and reinforcing rebars in the slab are assumed to behave like an elastic-plastic material with hardening both in compression and in tension and the Von Mises yield criterion is used. The steel grades S275 and A500 are used for structural elements and reinforcing rebars, respectively. Bolt steel is also modeled within the framework of Von Mises plasticity, but much higher strength (class 8.8) and limited ductility, obtained from the experimental data, are considered.

Numerical analyses and experimental tests showed that the behavior of the fuse was mainly dependent on the yielding and buckling of the steel plates and no major cracking of the slab was observed. Consequently, in numerical models concrete (class C30/37) was modeled with an elastic behavior, thus reducing the high computational demand, and buckling of the flange plate was properly simulated at hogging rotation.

In this study the finite element models are analyzed in terms of deformed shape and equivalent plastic strain (PEEQ) contour plot. The equivalent plastic strain is defined as follows:

$$PEEQ = \sqrt{\frac{2}{3}\varepsilon_{ij}^{p}\varepsilon_{ij}^{p}} \tag{3}$$

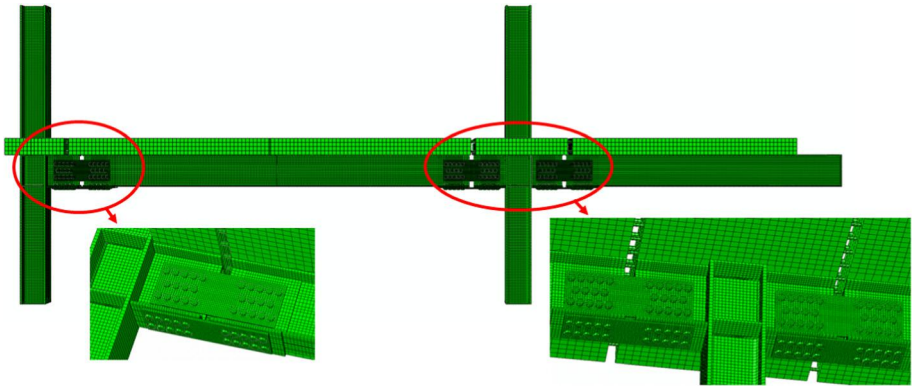

Fig. 6. FE model of a portion of a storey of a composite steel frame used for experimental tests carried out at Politecnico di Milano: plate B and free buckling length L_0 = 170 mm. Displacements are imposed at the top free edge of the columns. The column bottom edges are restrained with hinges.

It represents the equivalent plastic strain accumulated during the loading history.

Table 1 shows the dimensions and geometric slenderness of the bolted flange plates of the fuses used in the experimental tests and reproduced in the numerical models.

3.2. Numerical results

The results obtained from the numerical simulations carried out on the beam-to-column sub-assemblages are presented in this study. A displacement-controlled increasing (monotonic) loading history was applied at the free edge of the beam of the models, at a vertical distance of about 1450 mm from the center of the fuse device. Fig. 7 shows the deformed shape and the PEEQ contour plot at sagging and hogging rotations (top displacement imposed = 80 mm) for the models with different plates and free buckling length equal to 170 mm.

For sagging rotations, in all the models plastic deformations concentrate in the web and flange plates, ensuring that the plastic hinge occurs at the fuse section and protecting the remaining parts of the joint.

Reinforcing plates welded to the beam web near the connections are necessary to avoid the inelastic deformation of the beams. High PEEQ values are registered in the middle of the flange plates. This result is supported by the typical failure modes observed in the specimens tested in laboratory, consisting of the development of cracks at the mid-section of the flange plate under tension.

For hogging rotations, the results of the analyses indicate that both the column and the composite beam remained in the elastic range for all the different plates. The pronounced curved shapes of the plates show that the attempt of modeling the buckling behavior of the plates is achieved successfully. It is apparent that strength in the hogging configuration is controlled by buckling, which occurs as a function of both the geometric properties of the flange plates and the free buckling length of the fuse. The hogging resistance of the fuse is more sensitive to a geometry variation of the flange plates than sagging resistance. Buckling of the flange plate of the fuse is clearly observed for the models with plates D. In the models with plates C and B buckling of the fuse plate under hogging rotations is less evident.

When sagging and hogging behavior is compared, a more significant loss of stiffness, induced by buckling of the fuse plates, occurs under hogging rotation. The severity of yielding and buckling of the plates has a fundamental influence on the performance of the fuse device.

Fig. 8 shows the monotonic moment-rotation diagrams of the different bolted fuses obtained through the 3D FE models of the beam-to-column sub-assemblages (displacement imposed at the free edge of the beam = 60 mm). Under sagging rotation, plate C presents the highest moment capacity, while the lowest value is registered for plate D. Under hogging rotation, a marked reduction of the moment capacity is registered for plates D and A due to buckling of the flange plate. An enlargement of the flange plate cross-section causes an increase of both the resistant moment and the energy dissipation capacity of the fuse. However, it should be mentioned that large increases of the flange plate cross-section are not suggested because they may alter the strength hierarchy that prevents concentration of plastic deformation in the irreplaceable parts of the beam. The increase of the plate thickness mainly affects the behavior of the fuse under hogging rotation. The effects of the variation of the flange plate geometry are more evident under hogging rotation than sagging rotation.

The effects of different free buckling lengths were also investigated in the beam-to-column sub-assemblage models. Fig. 9 shows the PEEQ contour plot at sagging (left) and hogging (right) rotations (imposed top displacement = 80 mm) for the model with flange plate A and free buckling length equal to 140 mm. Comparing the results with those obtained from the model with the same plate and different free buckling length equal to 170 mm, it can be noted that buckling of the flange plate is less evident, plastic deformations are concentrated in a smaller region of the plates and higher PEEQ values are registered in the fuse device.

Fig. 10 shows the monotonic moment-rotation diagrams of the bolted fuses A and C for different free buckling lengths obtained through the 3D FE models of the beam-to-column sub-assemblages (displacement imposed at the free edge of the beam = 60 mm). As expected, an increase of the free buckling length causes a reduction of stiffness and moment capacity for both the fuses. It is worth noting that the variations are larger in the case of plate A than plate C: plate A presents higher values of geometric slenderness and it is more susceptible to buckling than plate C. The reduction of the moment capacity of plate A under hogging rotation is evident for high values of the free buckling length.

Fig. 11 presents the PEEQ contour plots in the models with plate A at sagging and hogging configurations at the onset of plastic deformations. In the model the plastic deformation involves some small parts of both the flange plate and the web plates. In both the cases of sagging and hogging rotations plastic deformations concentrate near the holes of the bolts in the web and flange plates.

The model of the bolted fuse device was then inserted in a portion of a composite steel frame in order to anticipate the behavior of the real scale specimen tested at Politecnico di Milano, Fig. 3. In the frame model the columns bottom edges were restrained with hinges and a displacement-controlled increasing (monotonic) loading history was imposed at the columns top edges, at a vertical distance of approximately 2800 mm from the column bottom edges. All the dimensions and geometrical details of the FE model are the same as the specimen tested at Politecnico di Milano and are reported in [16]. Fig. 12 shows both the deformed shape of the model of the frame sub-assemblage and the PEEQ contour plots near the beam-to-column connections. The results obtained with the frame sub-assemblage model confirm the outcomes observed in the beam-to-column sub-assemblage models. The objectives of the "Fuseis" research project are respected since all the potential damage is concentrated only in the fuses. A PEEQ concentration is registered in the device region, while both the column and the composite beam remain in the elastic range. Buckling of the flange plate can be observed in the internal beam-to-column connection at hogging rotation.

3.3. Comparison with experimental tests

Fig. 13 compares the numerical monotonic moment-rotation diagram, obtained through the 3D FE models of the beam-to-column sub-assemblages with plates D and B, with the experimental cyclic response derived from the corresponding test specimens. The loading history used in the experimental tests was based on a protocol similar to the one proposed by ECCS [29] and is reported in [17]. In the case of plate D, an overall satisfactory agreement can be observed between the numerical and experimental results. The FE model is able to accurately predict the experimental behavior, showing a good fit, especially in the elastic range and under hogging moment. It can be observed that slightly higher values of the moment resistance are registered in the numerical model under sagging rotation.

In the case of plate B, it can be noted that the FE model is much stiffer than the tested experimental specimen. It is worth mentioning that the specimen with plate B was experimentally tested later than the specimen with plate D. The poor agreement between numerical and experimental results could be therefore a consequence

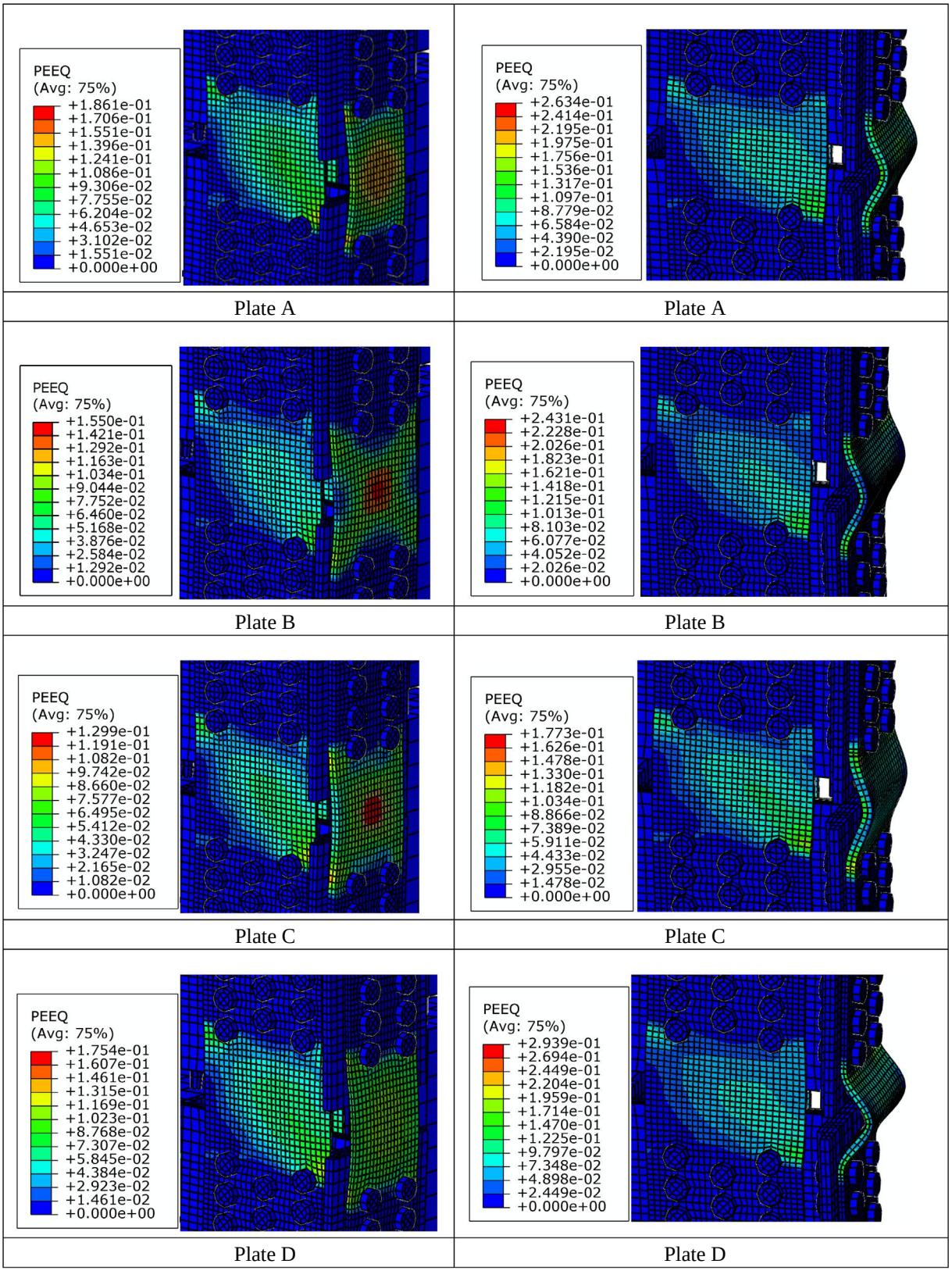

Fig. 7. PEEQ contour plot under sagging (left) and hogging (right) moment for the models with different flange plates (free buckling length L_0 = 170 mm). Displacement imposed at the free edge of the beam of the beam-to-column sub-assemblage model = 80 mm.

of the elastic stiffness loss shown by the specimens with plate B due to the damage accumulation in the irreplaceable parts of the specimen and to other low cycle fatigue effects.

Fig. 14 shows the failure modes of the experimental specimens with plates D and C for a comparison with the deformed shapes of the numerical models reported in Fig. 7. During the experimental

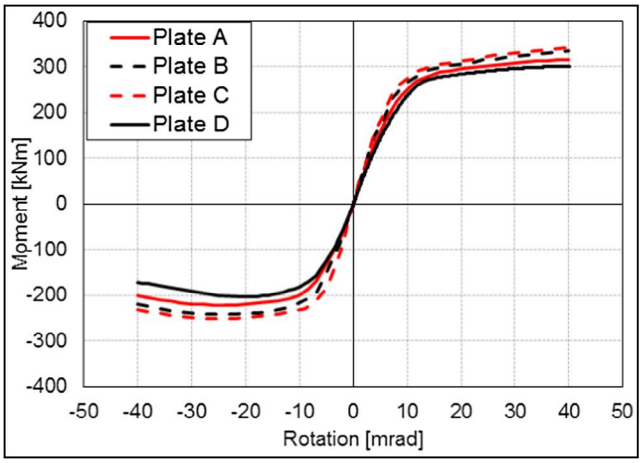

Fig. 8. 3D FE models of the beam-to-column sub-assemblage: moment-rotation diagrams of the different bolted fuses with free buckling length L_0 = 170 mm.

tests two main different failure modes of the fuses were observed. The fuse devices consisting of the thinnest plates were characterized by gross section failures after significant strength degradation due to buckling, as a result of hogging bending. In the case of flange plates with increased thickness, strength degradation due to buckling was not large enough to cause a gross section failure and net section failure was observed due to the lower cross-sectional area. The results of both numerical analyses and experimental tests highlight that the use of thin plates may be unsuitable for severe seismic actions, because the plates were prone to buckling and premature failures, as evidenced in Fig. 14 for plate D. Moreover, experimental results show that fuse devices exhibited larger rotations before significant strength degradation when net section failures occurred.

4. Development and calibration of simple models of the fuse devices

4.1. Numerical models

Numerical models of the test specimens were created by using the commercial code SAP2000 in order to develop simple models for the simulation of the seismic response of multi-storey composite steel frames with fuse devices. The first model consisted of a composite beam equipped with fuse devices connected to a column with the same geometry used in the experimental tests carried out at Instituto Superior Tècnico of Lisbon. The second model represented a portion of a composite steel frame with fuse devices with the same geometry used in the experimental tests carried out at Politecnico di Milano.

The beam was subdivided into different elements in order to take into account the presence of the fuse devices and the additional reinforcing steel plates near the gap section. The fuses were modeled as non-linear link elements with a length equal to the free buckling length of the fuses. The multi-linear plastic pivot model was used as hysteresis rule, including asymmetrical cross-section behavior with pinching and strength degradation. The link behavior was defined by a moment-rotation curve characterized by positive and negative moment capacities and initial stiffness of the fuse device. The initial input parameters of the monotonic moment-rotation diagram of the fuses were obtained from simplified analytical models described in [17]. The computation of the resistance and stiffness values for all the fuses was based on the material properties measured during the experimental campaign. The constitutive law adopted for the link was able to represent the plastic energy dissipation, the elastic stiffness, the ultimate moment and the stiffness and strength degradation of the fuse during the cyclic loading history used in the experimental tests, see Fig. 15.

4.2. Calibration procedure

The experimental results were used to calibrate and validate the numerical models in order to accurately predict the behavior of the fuses. All the numerical models of the beam-to-column sub-assemblages were subjected to the same cyclic loading history used in the experimental tests [17], with a maximum top displacement equal to 60 mm imposed at the free edge of the beam. The comparison between numerical and experimental diagrams is shown in Fig. 16 for the laboratory tests performed at Instituto Superior Tècnico of Lisbon. As can be noted, a good agreement is achieved in terms of moment capacity, elastic stiffness, energy dissipation and pinching behavior. The overall joint behavior is characterized by inelastic deformations taking place in the fuse system that prevents the formation of plastic hinges at the end of the beam. The asymmetry of the diagram in terms of bending moment is due to the presence of the concrete slab and to the strength loss caused by buckling of the fuse plates when under hogging rotation. The maximum rotation observed in the fuse device is about 40 mrad. The deformation capacity of the fuses was demonstrated by the experimental tests where all the specimens were able to achieve rotations of about 40 mrad.

Fig. 17 shows the comparison of the numerical and experimental moment-rotation diagrams of the fuses for the laboratory tests performed at Politecnico di Milano. All the numerical models of the frame sub-assemblages were subjected to the same cyclic loading history used in the experimental tests [16]. The diagrams show

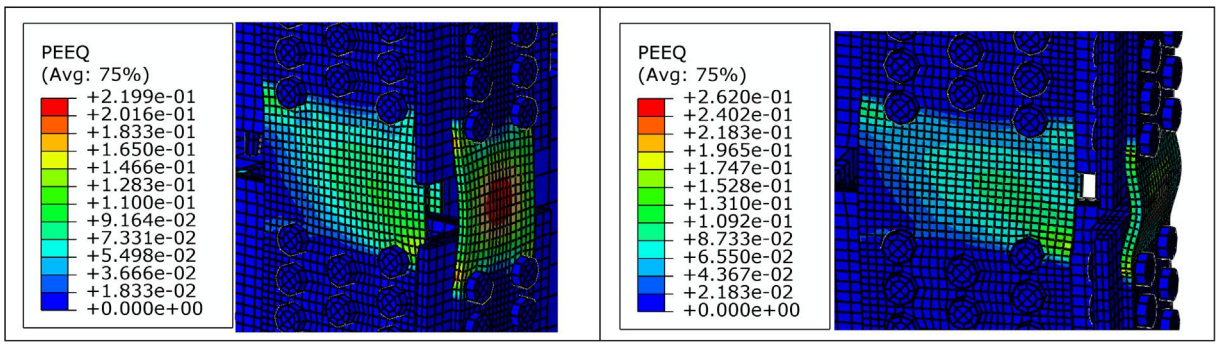

Fig. 9. PEEQ contour plot under sagging (left) and hogging (right) moment (displacement imposed at the free edge of the beam of the beam-to-column sub-assemblage model = 80 mm) for the model with plate A and free buckling length L_0 = 140 mm.

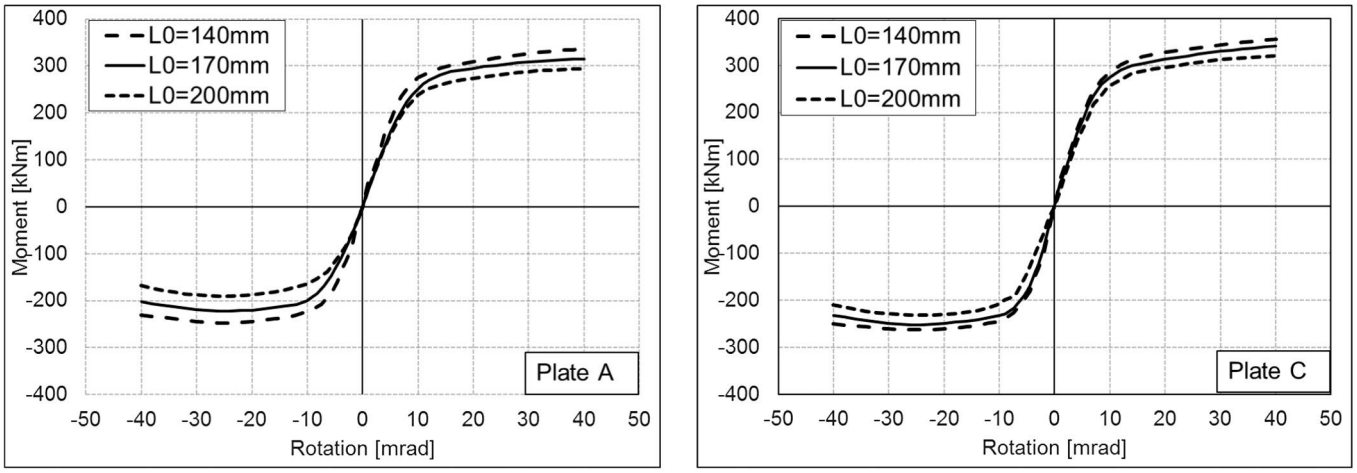

Fig. 10. 3D FE models of the beam-to-column sub-assemblage: influence of different free buckling lengths on the moment-rotation diagrams of the bolted fuses A and C.

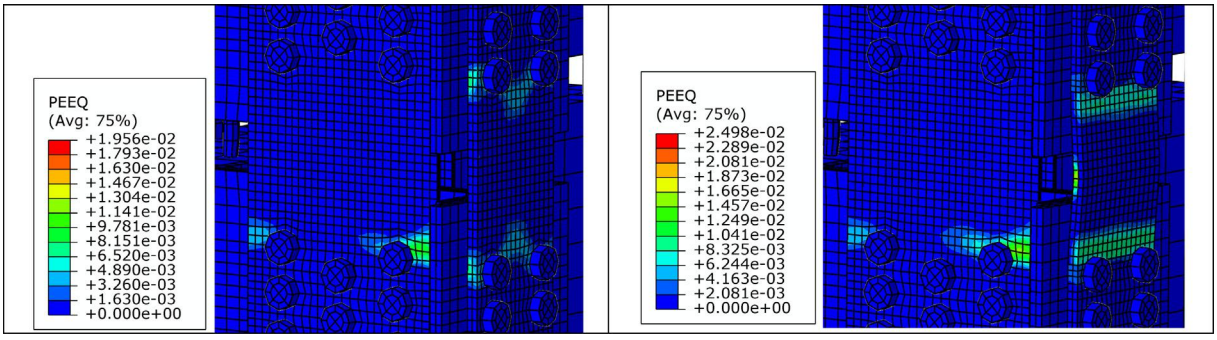

Fig. 11. PEEQ contour plot under sagging (left) and hogging (right) moment at the onset of plastic deformations for the FE model with plate A (free buckling length L_0 = 170 mm).

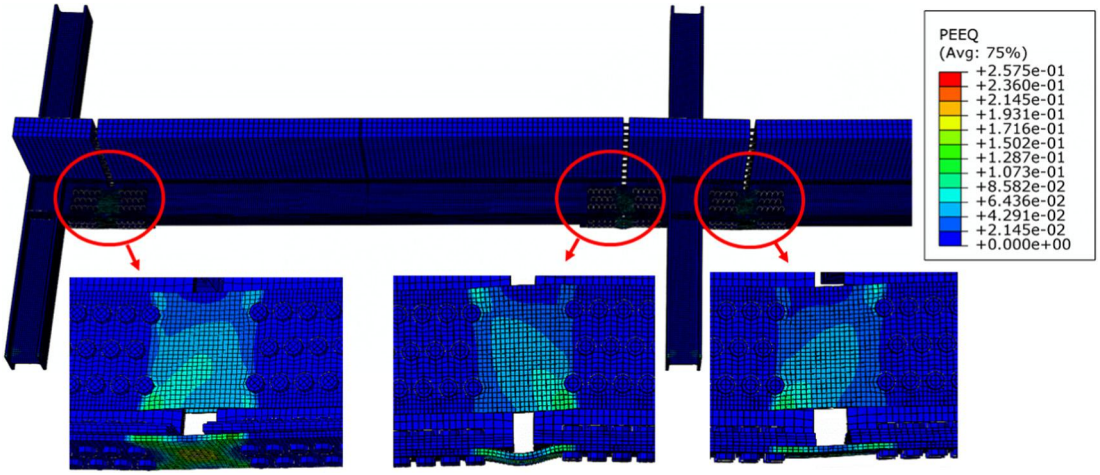

Fig. 12. Deformed shape of the frame sub-assemblage model and PEEQ contour plots in the bolted fuses (displacement imposed at the top edge of the column = 80 mm).

that the hysteretic behavior of the fuses is stable, characterized by a marked pinching phenomenon due to the slippage of the bolts and to the buckling of the fuse plates.

The values of the resistance capacity ratio and elastic stiffness of the fuses utilized in this study, for sagging and hogging rotations, are reported in Fig. 18. Plates B and C exhibit higher moment resistance than the other tested plates because of their larger resistant sections. As regards the elastic stiffness, it was decided to adopt the values of the initial stiffness that more accurately approximate the experimental results for the following numerical analyses on multi-storey composite steel frames.

After the calibration of the numerical models with the results of the experimental tests, another moment-rotation curve, hereafter denoted as plate M, was considered for the bolted fuse devices. Such a plate presents the highest values of resistance capacity ratio and elastic stiffness for sagging and hogging rotations. The input

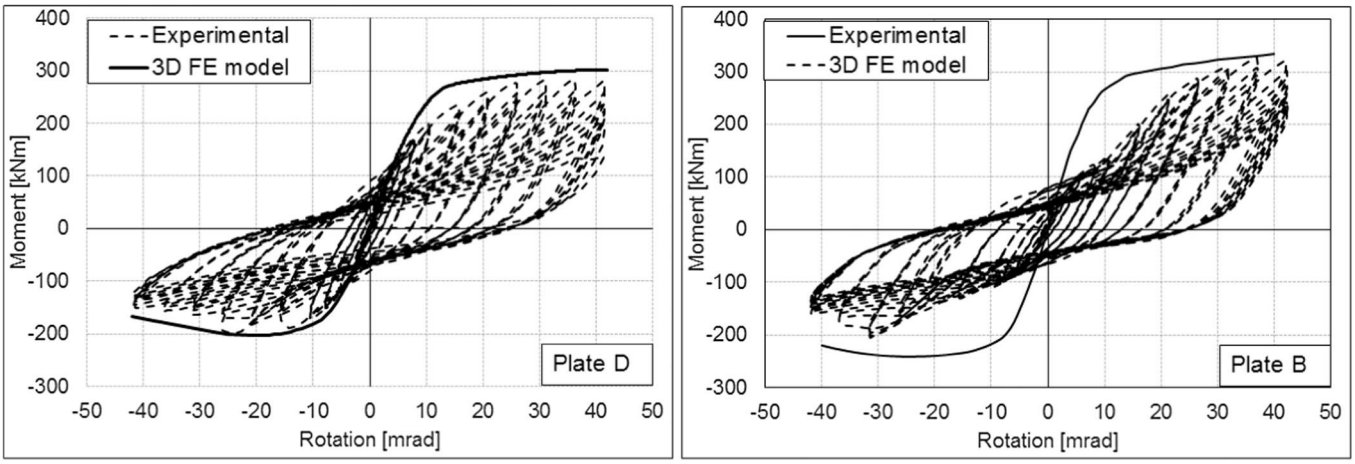

Fig. 13. Moment-rotation diagrams for fuse devices with plates D and B (free buckling length L_0 = 170 mm): comparison between 3D FE models and experimental tests.

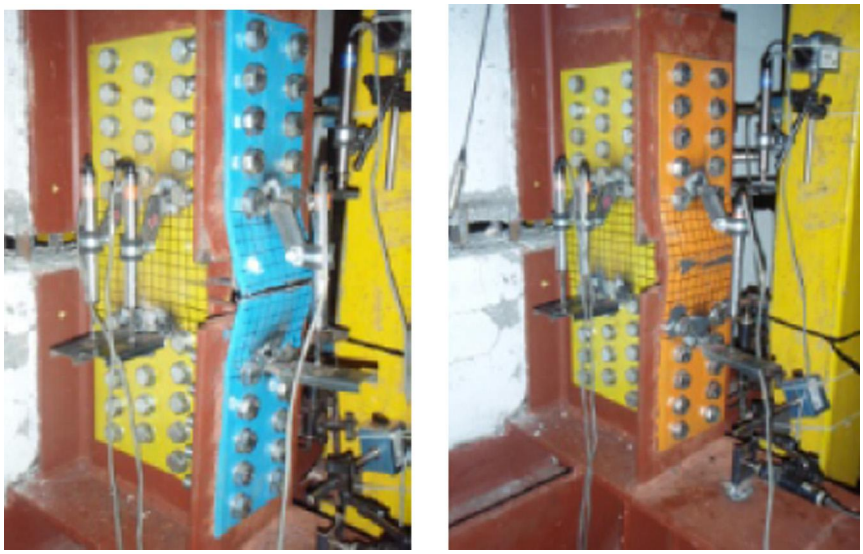

Fig. 14. Failure modes of the flange plates of the fuse device observed in the experimental tests at Instituto Superior Tècnico of Lisbon: plate D (thin plate) and plate C (thick plate) with free buckling length L_0 = 170 mm.

parameters of the monotonic moment-rotation curve for plate M were obtained from the 3D FE models. The main geometrical characteristics assumed for the flange plate of the 3D FE model with plate M were: thickness = 14 mm, width = 170 mm, geometric slenderness = 12.1. It is worth mentioning that the initial mechanical characteristics of plate M were not affected by the deterioration of the specimen sub-assemblages observed for other plates during the experimental tests. The numerical moment-rotation diagram assumed for plate M and the monotonic curve derived from the 3D FE model are shown in Fig. 19. Moreover, Fig. 19 compares the numerical moment-rotation curve of plate M with the moment-rotation curves of the other plates obtained through the simplified models of the beam-to-column sub-assemblages under the loading history used in the experimental tests [17].

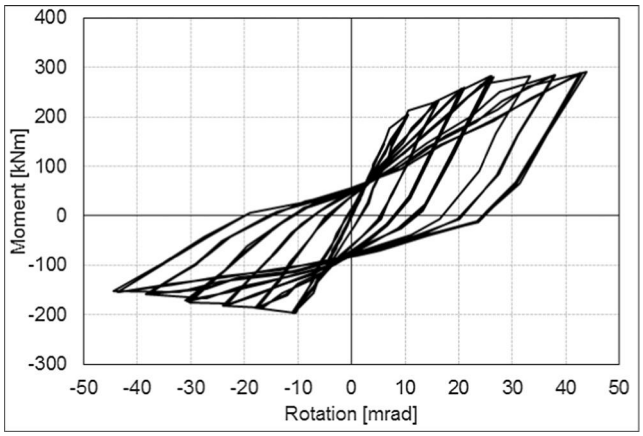

Fig. 15. Numerical moment-rotation diagram of a fuse (plate D).

The simplified models proved to be able to accurately represent the actual behavior of the fuses. It is worth mentioning that the moment-rotation curves of the simplified models were obtained using initial parameters derived from analytical design models described in [17] and then calibrated through the results of the experimental tests. The same analytical design models described in [17] can be used to derive the joint properties in order to extend the results to different types of joints and fuses that may vary in

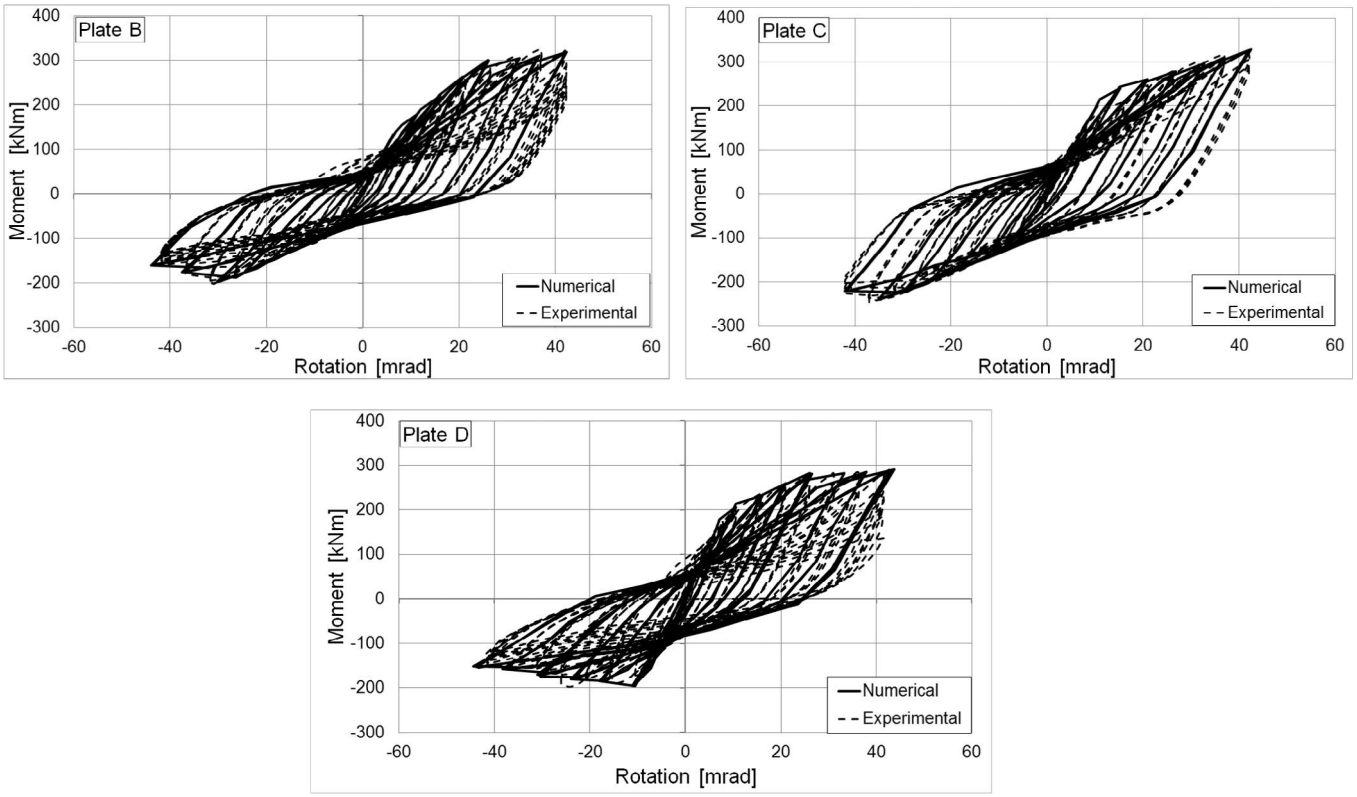

Fig. 16. Experimental and numerical moment-rotation diagrams of the bolted fuses tested at Instituto Superior Tècnico of Lisbon (free buckling length L_0 = 170 mm).

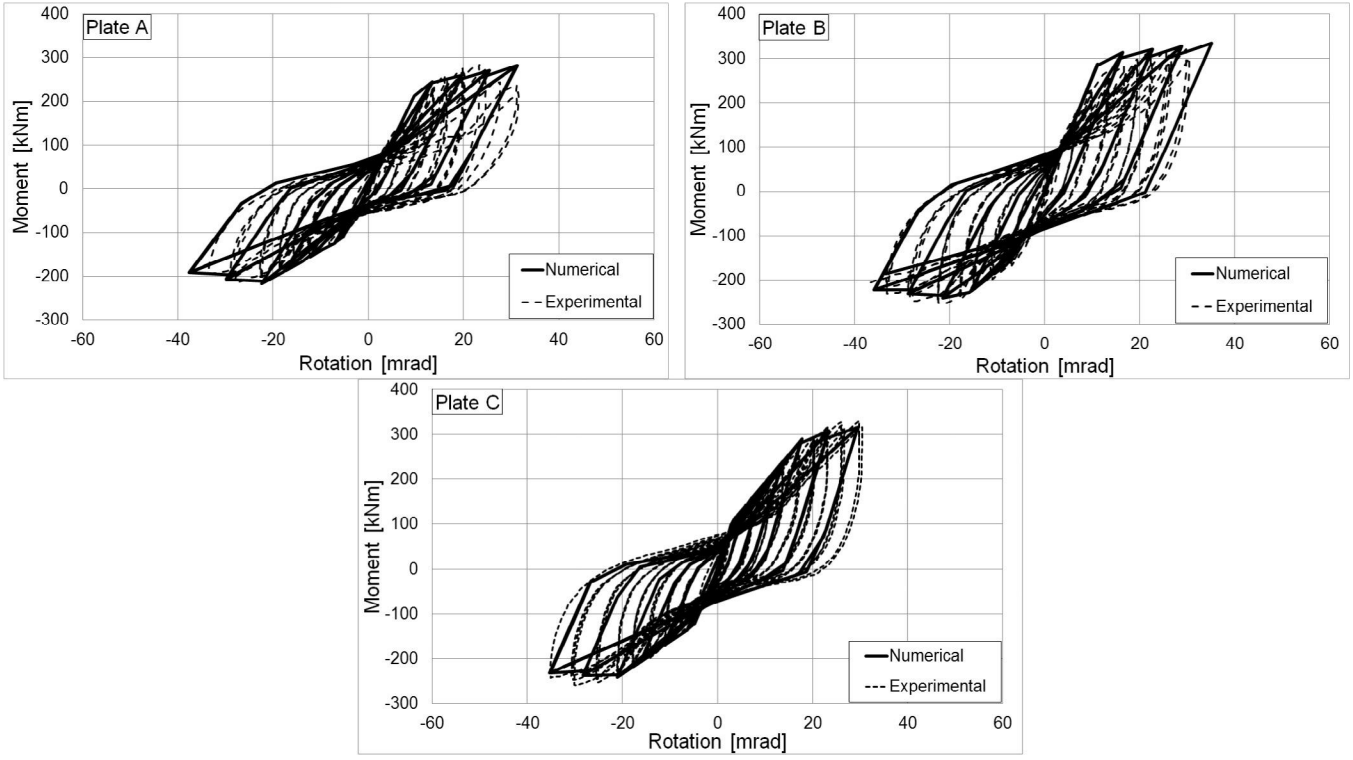

Fig. 17. Experimental and numerical moment-rotation diagrams of the bolted fuses tested at Politecnico di Milano (free buckling length L_0 = 170 mm).

terms of geometrical and mechanical characteristics. The proposed analytical models allow the computation of the moment resistance and stiffness of the fuses from the geometrical and mechanical parameters (dimensions of the elements and steel grade).

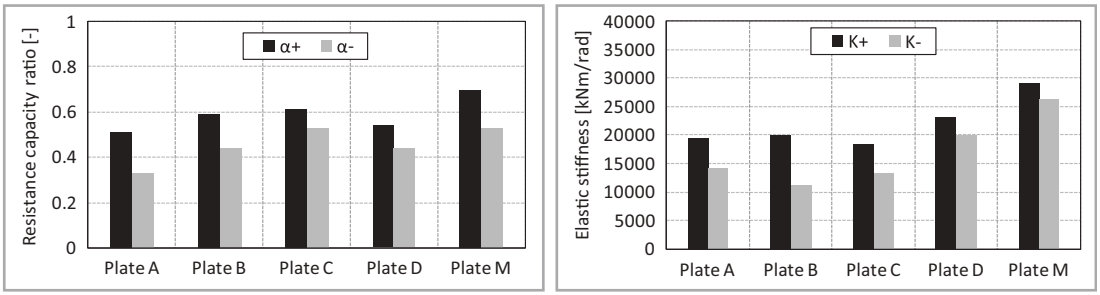

Fig. 18. Resistance capacity ratio and elastic stiffness under sagging (positive) and hogging (negative) rotations for the different plates (free buckling length L_0 = 170 mm).

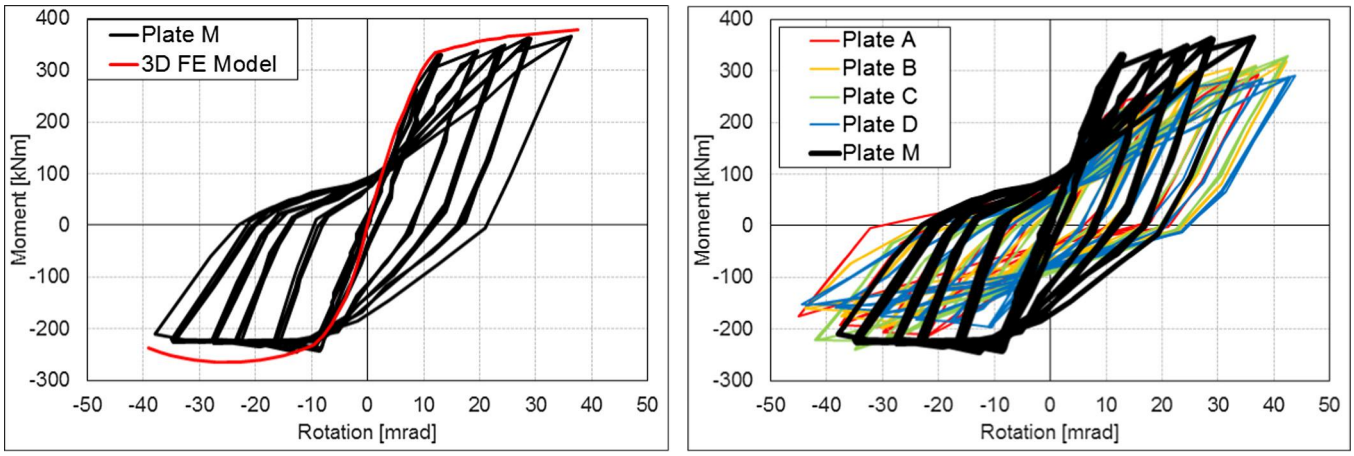

Fig. 19. Moment-rotation diagram of the bolted fuse with plate M: comparison with the 3D finite element model and with other fuses (free buckling length L_0 = 170 mm).

5. Steel frames and numerical models

5.1. Steel frames under study

In order to extend the results of the numerical analyses carried out on the models of the test specimens to multi-storey frames under seismic excitation, non-linear dynamic analyses are performed on moment-resisting composite steel frames equipped with fuse devices. The main aims are: (1) to analyze the seismic response of steel frames with fuse devices near the beam-to-column connections for various ground motion intensity levels; (2) to evaluate the contribution of the fuse devices to the energy dissipation of multi-storey frames; (3) to assess the influence of the main mechanical and geometrical characteristics of the different devices on the seismic performance of several steel frames.

The set of multi-storey frames under study (denoted as F2) consists of three frames with five bays and different number of storeys ranging from three to nine. The frames are considered as part of composite steel buildings and are supposed to be spaced 6 m one from another. The height of each storey is 3.5 m, while the width of each bay is 6 m. The beams are composite sections made by IPE300 section profile and a 15 cm thick concrete slab, whereas the dimensions of the column sections change as a function of the number of the storeys of the frame. The same cross-sections of the test specimens are used for the composite beams of the multi-storey frames in order to reproduce the findings obtained in the experimental campaign. Steel grade of the structural members is assumed to be S275. A schematic representation of the geometric dimensions of the frames with section profiles for columns and beams is reported in Fig. 20. The benefits of the insertion of the fuse devices in composite steel frames are evaluated by comparing the seismic response of both conventional frames and innovative frames equipped with fuse devices.

5.2. Numerical models

Numerical models of both conventional steel frames without fuse devices and innovative seismic resistant steel frames with fuse devices were developed using the computer code SAP2000. Hereafter, conventional frames are denoted as “F2-n” and innovative frames are denoted as “F2Pi-n”, where n and i indicate the number of the storeys of the frame and the type of plate used in the model, respectively.

A lumped plasticity modeling approach was employed for the non-linear models of the frames. Beam and column elements were modeled as frame elements and non-linearity was concentrated in plastic hinges at their ends. To characterize the non-linear behavior of a plastic hinge, the force-displacement properties suggested in FEMA 356 [24] were implemented. For the beams flexural moment hinges were considered, while plastic hinges accounting for the interaction between axial force and bending moment were defined for the columns. Beam-to-column joints were considered as rigid in accordance with the connection detailing of the experimental tests. The length of the beams was subdivided into different elements in order to take into account the presence of the fuse devices and the additional steel reinforcement in the gap section.

The models of the different fuse devices were implemented in the numerical models of the frames. The fuses were modeled as non-linear link elements inserted in the beams with a length equal to the free buckling length of the bolted plates. The multi-linear plastic pivot model was used as hysteresis rule for the fuses. The values of the parameters used for the hysteretic model were those

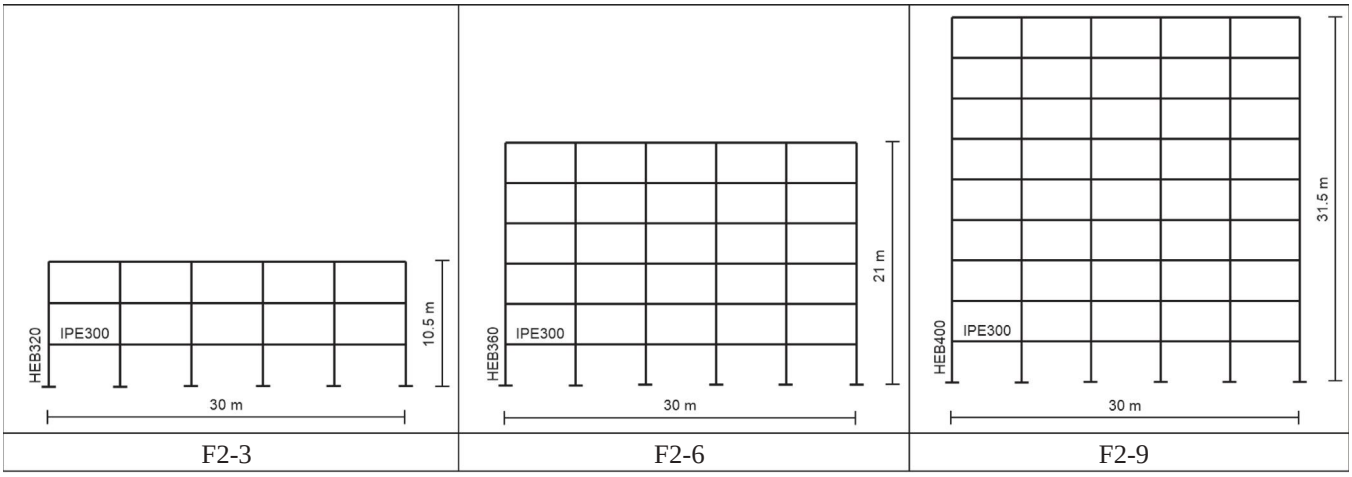

Fig. 20. Steel frames under study.

obtained from the calibration of the models of the specimens tested at Instituto Superior Tècnico of Lisbon.

The additional steel reinforcement in the gap section was reproduced in the numerical models by adding different cross-sections and plastic hinges properties around the device. The length of these regions was assumed in the model in accordance with the geometry of the experimental specimens.

6. Numerical analyses and results

The seismic performance of the composite steel frames under study was assessed through non-linear dynamic analyses with response spectrum-compatible artificial accelerograms. The set of artificial ground motions consisted of three different records that were generated so as to match the Eurocode 8 response spectrum (Type 1, soil type A, 5% viscous damping) through the computer code SIMQKE [25]. Fig. 21 shows the response spectra of the artificial accelerograms used in this study. The numerical analyses were performed for three different ground motion intensity levels characterized by peak ground accelerations (PGA) between 0.3 g and 0.7 g. Non-linear static (pushover) analyses were also performed in order to detect potential damage localization, to assess the distribution of plastic hinges and to evaluate the attainment of failure mechanisms.

6.1. Top displacement and base shear

The results of the non-linear dynamic analyses in terms of maximum roof displacement and base shear are presented using the average values of the results obtained using three artificial records. The maximum top displacements of the different frames are shown in Fig. 22 for different peak ground accelerations. As can be noted, the maximum top displacements of the innovative frames with fuses are generally larger than those of the conventional frames because the insertion of the fuse devices has the main consequence of reducing the lateral stiffness of the frames. Eigen-value analyses confirm that innovative seismic resistant steel frames with fuse devices are more flexible and present larger values of fundamental periods than conventional frames. The results of non-linear dynamic analyses show that the maximum top displacements of frames F2PM are very close to those of the conventional frames, above all under ground motions with PGA = 0.7 g.

Comparing the seismic performance of the different innovative frames, it is interesting to note that the initial stiffness and resistant moments adopted for the constitutive laws of the fuse devices

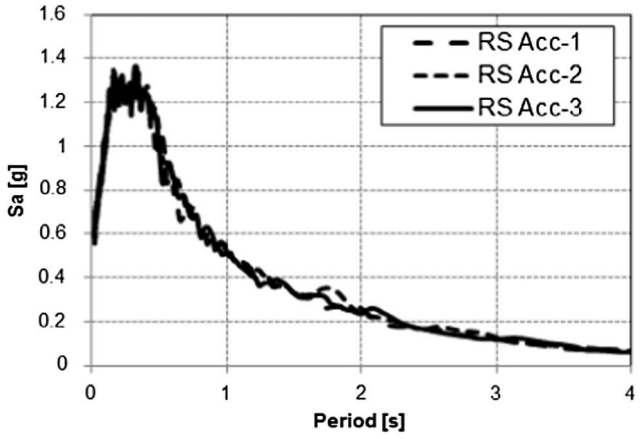

Fig. 21. Response spectra of the artificial accelerograms.

affect the results. For smaller values of seismic intensity levels (PGA = 0.3 g), frames F2PM exhibit the smallest top displacements (the moment-rotation curve adopted for the fuse M presents the highest elastic stiffness). For higher values of seismic intensity levels (PGA = 0.7 g), frames F2PM, F2PB and F2PC present the smallest top displacements (the moment-rotation curves adopted for the fuse plates M, B and C present the highest resistant moment).

As can be observed, in all the examined cases the increase of top displacement is evident for decreasing values of the mechanical characteristics of the fuse (initial stiffness and resistant moment). A significant reduction of the mechanical characteristics of the fuse (Fuse A and D) can be detrimental to the seismic performance of the innovative frames in terms of top displacements.

The maximum values of the base shear of the frames, reported as average values of the ones obtained by the non-linear dynamic analyses using three accelerograms, are shown in Fig. 23 for different peak ground accelerations. It can be noted that the peak values of the base shear of the frames with fuses are always smaller than those of the conventional frames. The decrease of the base shear depends mainly on the resistance capacity ratio of the fuse devices. The frames equipped with fuses with the highest resistant moments (frames FPM, FPB and FPC) exhibit the largest values of the base shear, while the reduction of the base shear is more evident in the case of frames F2PA and F2PD.

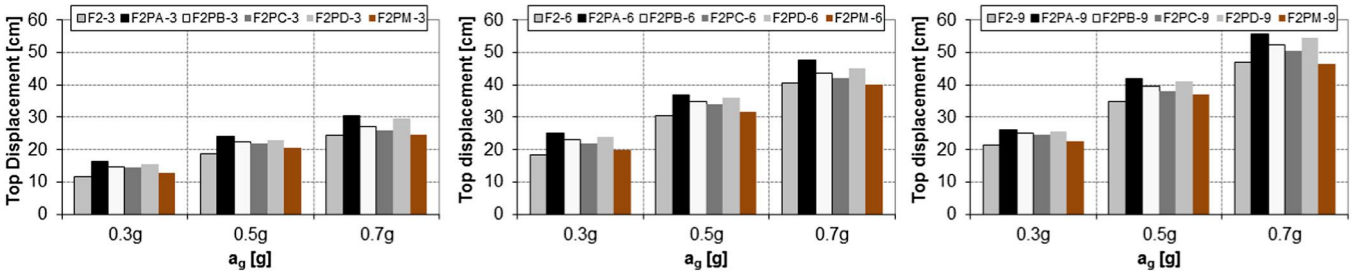

Fig. 22. Maximum top displacements of the conventional frames F2 and innovative frames with fuses F2P for different peak ground accelerations.

6.2. Plastic hinge pattern and energy dissipation

The plastic hinge distribution for conventional and innovative frames is assessed through non-linear dynamic analyses. Although the number and distribution of plastic hinges are very similar for the two types of frames, some differences can be highlighted.

In conventional frames plastic deformations generally occur at the beam ends and at the base of the ground level columns, reflecting the design of the frames according to the provisions of Eurocode 8 [27,28]. Nevertheless, for high values of PGA some plastic hinges are sometimes observed also at the columns ends of different storeys.

Innovative frames with fuse devices guarantee a better control of plastic mechanism than conventional frames at high levels of seismic action. In fact, in all the examined cases the application of the fuse devices prevents the formation of plastic hinges in columns, except at the columns base. In innovative frames plastic deformations concentrate only in the fuses and the beam ends are protected remaining in the elastic range. The fuses act as dissipative devices, thus avoiding the formation of plastic deformations into the columns and minimizing the repair costs even though the initial costs of construction may be higher than those for conventional frames. Moreover, numerical results show that no kinematic mechanism is observed for all the frames under study subjected to severe seismic excitations with PGA = 0.7 g.

The difference in the plastic energy dissipation of conventional and innovative frames is investigated too. Fig. 24 compares the amount of plastic energy dissipated in conventional and innovative frames with different plates under PGA = 0.7 g, considering columns, beams and fuses separately. As can be observed, the total amount of hysteretic energy dissipated in innovative frames with fuses is higher than in conventional frames. This result can be explained by the higher values of hysteretic energy dissipated by fuses in innovative frames than by beams in conventional frames. The plastic deformation demand in columns decreases slightly when fuse devices are present.

The influence of the resistance capacity ratio of the fuses on the plastic energy dissipated in innovative frames with different plates is also assessed. Frames F2PM dissipate the largest amount of plastic energy for all the structures. As can be observed in Fig. 19, plate M presents large hysteretic cycles with negligible pinching effects. Frames F2PA and F2PD show the smallest amount of plastic energy dissipated in fuses among the innovative frames. Numerical results confirm that the plastic deformation demand in fuses and columns is affected by the resistance capacity ratio of the fuses.

Fig. 25 shows the plastic energy dissipated in conventional frames and in innovative frames F2PM for different peak ground accelerations. At lower ground motion intensity levels, the innovative frames dissipate small amounts of plastic energy in fuses, whereas the conventional frames practically remain in the elastic range. Innovative frames yield and start dissipating plastic energy earlier than conventional frames due to their lower stiffness and strength. For each level of PGA, the energy dissipated by fuses in innovative frames is larger than that dissipated by beams in conventional frames. Moreover, the plastic energy dissipated in columns is slightly smaller in innovative frames than in conventional frames.

As well known, the global ductility of the frames significantly depends on available local ductility. High inelastic deformations and large amounts of plastic energy dissipation require high values of rotation capacity of the plastic hinge regions. Fig. 26 shows the maximum values of rotations computed in beams and fuses of the first storeys for the different frames under PGA = 0.7 g. As can be noted, the maximum rotations registered in fuses of innovative seismic-resistant frames are larger than in beams of conventional frames. The deformation capacity of the fuses was demonstrated by the results of the experimental tests carried out both at Instituto Superior Tècnico of Lisbon and at Politecnico di Milano. The specimens showed stable hysteresis loops and were able to achieve rotations equal to 35 mrad. The maximum values of the rotations attained by the fuses of the frames in non-linear dynamic analyses were about 35 mrad, a value for which the fuses of the experimental tests showed good energy dissipation capacity.

6.3. Maximum and residual interstorey drift ratio

Peak roof displacements provide an indication of the global response of the structure, while the peak and residual interstorey drifts can be related to potential structural and non-structural

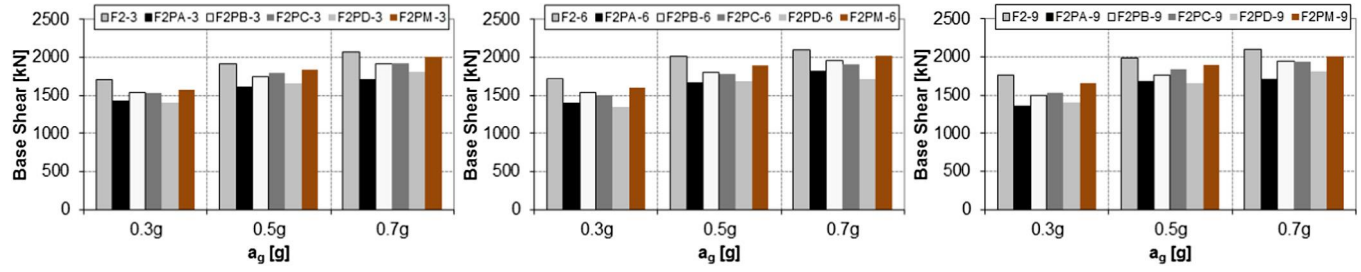

Fig. 23. Maximun values of the base shear of the conventional frames F2 and innovative frames with fuses F2P for different peak ground accelerations.

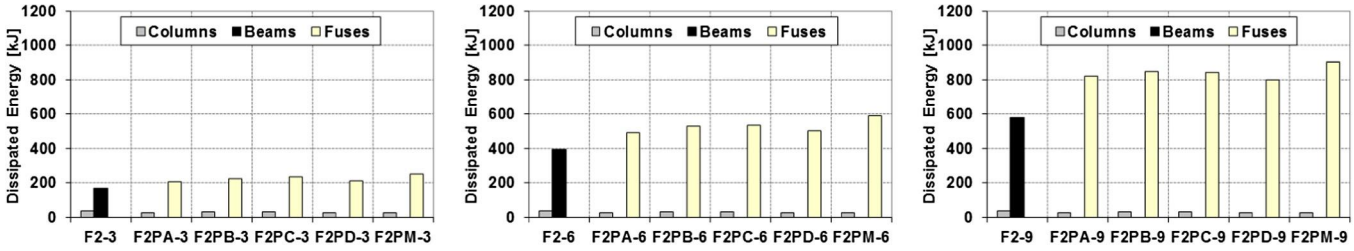

Fig. 24. Plastic energy dissipated in conventional frames F2 and innovative frames with fuses F2P under PGA = 0.7 g.

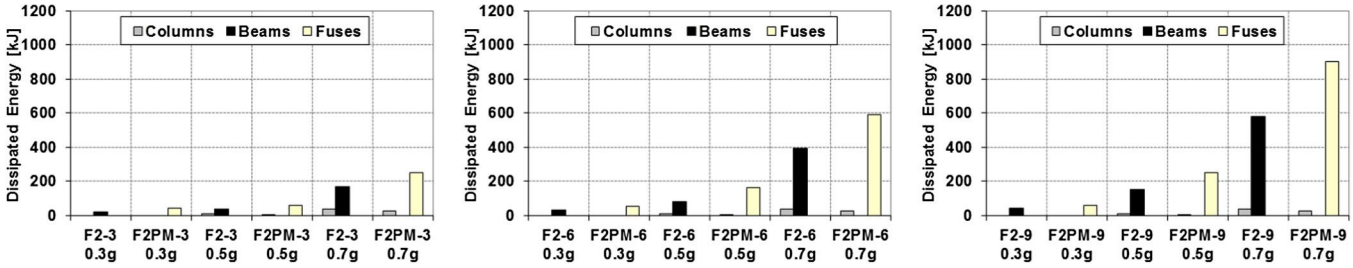

Fig. 25. Plastic energy dissipated in conventional frames F2 and innovative frames F2P with fuse M for different peak ground accelerations.

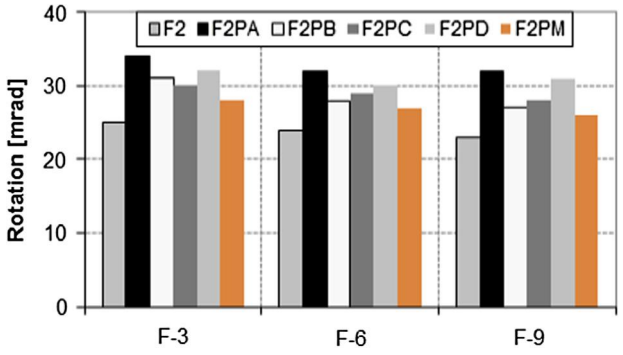

Fig. 26. Maximum rotation in beams and fuses for conventional (F2) and innovative (F2P) frames under PGA = 0.7 g.

damage. Fig. 27 shows the maximum interstorey drift ratio (IDR) of the conventional and innovative frames for different peak ground accelerations: the interstorey drift ratio is defined as the difference in lateral displacements between two consecutive floors normalized by the interstory height. The maximum IDR values of the innovative frames with fuses are generally larger than those of the conventional frames: the maximum IDR values are registered for frames F2PA. It can be noted that frames F2PM exhibit similar IDRs as the conventional frames.

It is worth mentioning that the maximum IDR of the different frames is generally registered at different storeys (1^{st}-2^{nd} storeys for the three-storey frames, 2^{nd}-4^{th} storeys for the six-storey frames, 4^{th}-6^{th} storeys for the nine-storey frames). Moreover, numerical results show that the critical storeys may change as a function of the peak ground acceleration. It can be noted that the innovative frames generally exhibit the maximum IDR at upper storeys than the conventional frames.

Residual drifts are the permanent deformations of a structure that remain at the end of a seismic excitation and they are caused by the non-linear behavior of the yielding components in the system. Typically, residual drifts tend to be significantly lower than maximum drifts, but they can achieve significant values. Large residual drifts can be a potential drawback of conventional frames and provide useful information on the damage level and on the post-earthquake repairability of the frames.

The residual drift ratio is computed at the end of the numerical simulations for all the frames under study and the results obtained under PGA = 0.7 g are reported in Fig. 28. The values of the residual drift ratio are lower than the limit of 0.5% for all the frames. The highest values are registered for the conventional frames. Numerical results show a decrease of the residual drift ratio with the increase of the mechanical characteristics of the fuses. Innovative frames with plate M experience smaller residual drifts than the other frames, thus allowing for an easy repair after the earthquake.

6.4. Overall ductility factor

Non-linear static (pushover) analyses were performed in order to estimate the damage distribution and the expected plastic collapse mechanism of the different frames. Pushover analyses were carried out applying two types of lateral load distribution: the first proportional to the first mode and the second proportional to the masses along the frame height. Numerical results confirm the reduction of the lateral stiffness of the innovative frames with fuses when compared with conventional frames and the global failure mechanisms observed in non-linear dynamic analyses.

The overall ductility factor μ is computed for all the frames in order to evaluate the plastic displacement capacity that innovative frames with fuses can provide until the achievement of the plastic mechanism. The ductility factor μ is defined as the ratio between the roof displacement δ_u when a plastic mechanism is achieved and the roof displacement δ_y associated with the formation of the first plastic hinge. Fig. 29 shows the overall ductility factors obtained from pushover analyses using both the first mode and uniform distributions (more conservative results are reported). Conventional frames generally exhibit smaller values of the overall ductility factor than innovative frames with fuses. The maximum values of the overall ductility factor are registered for innovative frames with plate M. As can be noted, three-, six- and nine-storey frames exhibit similar values of the overall ductility factor.

6.5. Effects of different locations of the fuse devices

The efficiency of the fuse devices depends on proper design rules, which include both the location and the resistance capacity

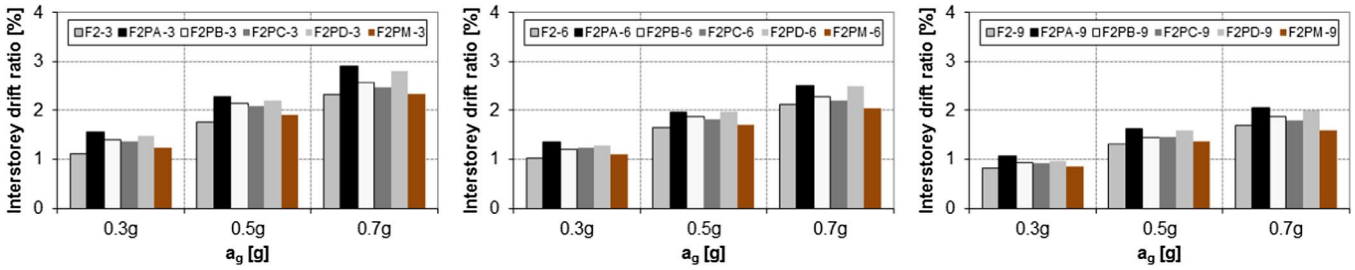

Fig. 27. Maximum interstorey drift ratio of the conventional frames F2 and innovative frames F2P for different peak ground accelerations.

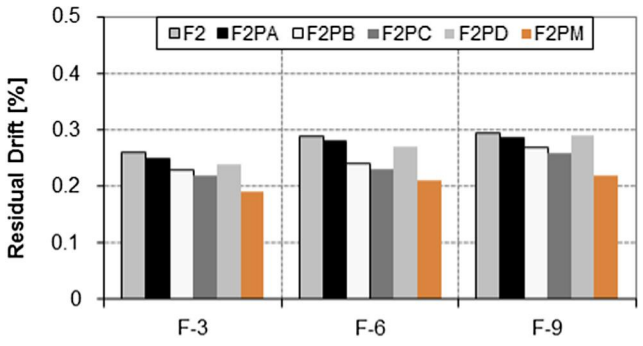

Fig. 28. Residual drift ratio of the conventional (F2) and innovative (F2P) frames under PGA = 0.7 g.

ratio of the fuse. The effects of three different locations of the fuse devices on the seismic response of the innovative frames were investigated for the six-storey frames with plates A, C and M. Numerical models of the frames with different distances of the fuse (L_1 = 25 cm, L_2 = 35 cm, L_3 = 50 cm) from the column flange were created and investigated through non-linear dynamic analyses. The results of the numerical simulations confirm that the location of the fuse device is an important design parameter influencing the seismic response of the frames. When the distance of the fuse measured from the column flange increases, the top displacement generally decreases and the base shear increases, as shown in Figs. 30 and 31. Moreover, the formation of the first plastic hinges in the fuse devices is deferred and occurs early at the columns base. The total amount of the plastic energy dissipated by the frames generally decreases when the distance of the fuse increases.

However, it is necessary to avoid too large distances of the fuses from the column flange, since damage would be more easily concentrated in the irreplaceable parts of the frame, such as beams and columns, than in the dissipative devices. Fig. 32 shows a decrease of the plastic energy dissipated in fuses and the appearance of damage in beams for the case of distance equal to L_3 = 50 cm. In fact, the energy supplied by severe earthquakes in the case of innovative frames with distance of the fuse equal to L_3 = 50 cm is dissipated not only by the hysteretic behavior of the fuses, but also through a plastic damage of the beams and beam-to-column connections. Moreover, the plastic rotation demand at the base of the ground level columns is affected by the position of the fuse devices too.

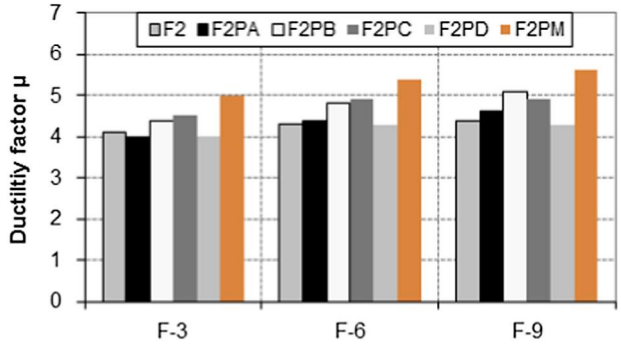

Fig. 29. Values of the overall ductility factor for conventional (F2) and innovative (F2P) frames.

The seismic behavior of three innovative frames as a function of the different distances of the fuses from the column flange is described in detail hereafter.

6.5.1. Frame F2PA

In the case of distance of the fuse equal to L_1 = 25 cm, frame F2PA exhibits a large increase of top displacements, above all under severe seismic excitation (PGA = 0.7 g). The beams are protected from damage, but the plastic energy dissipated by the fuses is smaller than the other frames because of pinching effects and buckling of steel plates. The plastic energy dissipated by columns is slightly higher than the other frames. The decrease of base shear is evident for all the positions of the fuses when compared with conventional frame. The best seismic performance is obtained in the case of distance of the fuse equal to L_3 = 50 cm; although a small damage is registered in the beams, there is a large reduction of top displacements and the decrease of energy dissipation of the fuses is limited when compared with the case of L_1 = 25 cm. Numerical analyses show that the values of top displacements of frame F2PA are very sensitive to the location of the fuses.

6.5.2. Frame F2PC

The seismic behavior of frame F2PC is similar to that of frame F2PA, but the values of top displacements are smaller and less sensitive to the position of the fuses. The best results are obtained in the case of distance of the fuse equal to L_2 = 35 cm and L_1 = 25 cm; the energy dissipation of the fuses is satisfactory and beams are protected from damage. However, in the case of L_1 = 25 cm, frame F2PC exhibits a detrimental increase of top displacements when compared with the other fuses locations. In the case of L_1 = 50 cm, beams are not protected from damage. A decrease of the base shear is observed with the reduction of the distance of the fuse.

6.5.3. Frame F2PM

A satisfactory seismic performance of frames F2PM is obtained in the case of L_2 = 35 cm and L_1 = 25 cm. In the case of L_3 = 50 cm, a large decrease of the energy dissipated by the fuse is observed because fuse M presents the highest moment resistance. Consequently, a non-negligible amount of plastic energy dissipated by beams is registered, indicating that the beams are not protected from damage. However, the plastic energy dissipation of fuses is satisfactory because pinching effects are limited. The plastic energy dissipated by columns slightly increases for L_3 = 50 cm. Numerical analyses show that the values of top displacements obtained using

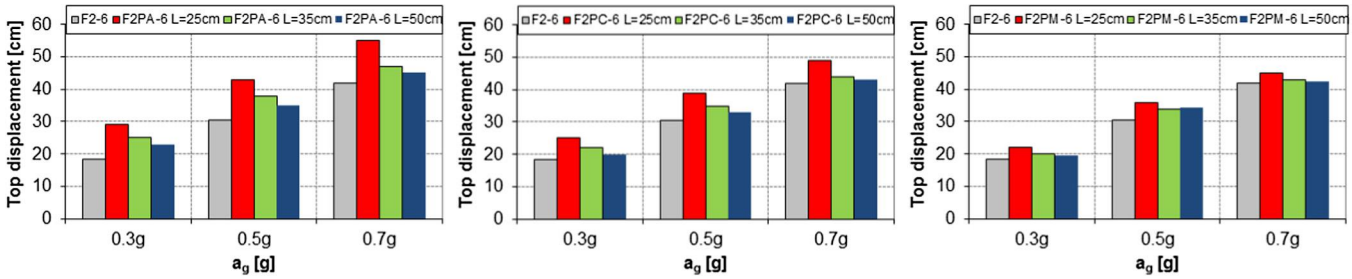

Fig. 30. Maximum top displacements of six-storey frames (F2, F2PA, F2PC, F2PM) with different fuses locations for various ground motion intensity levels.

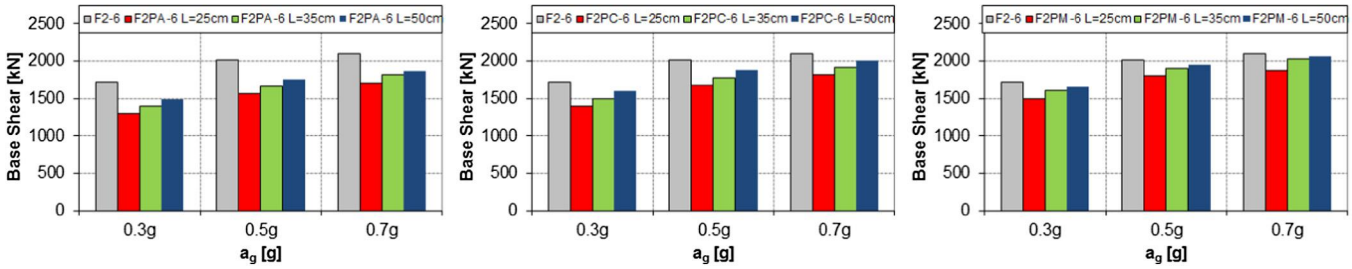

Fig. 31. Maximum values of the base shear of six-storey frames (F2, F2PA, F2PC, F2PM) with different fuses locations for various ground motion intensity levels.

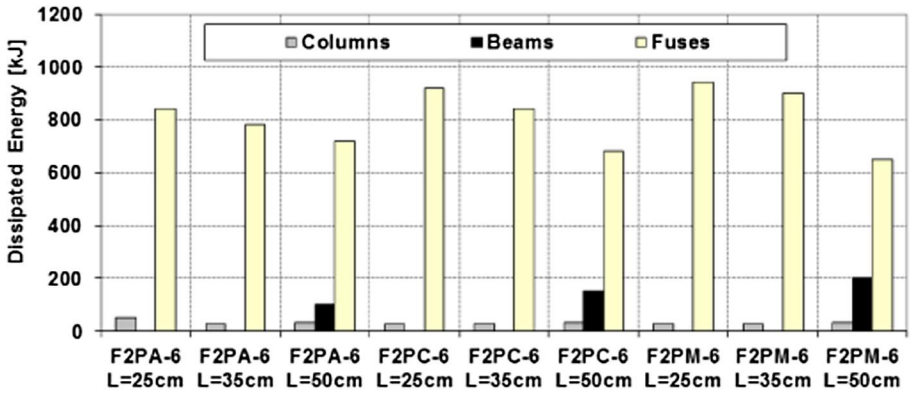

Fig. 32. Plastic energy dissipated in six-storey frames (F2PA, F2PC, F2PM) with different locations of fuses under PGA = 0.7 g.

fuse M are less sensitive to the position of the fuse than the other cases. Moreover, the maximum top displacements of frames F2PM are generally smaller than those of the frames with other fuses and the variation of the base shear is limited when compared with conventional frame.

It is apparent that the location of the fuse should be chosen as a function of the resistance capacity ratio of the device. When dealing with fuse A, the distance L_1 = 25 cm should be avoided because large top displacements of the frames can be observed. In the case of fuses C and M, the distance L_3 = 50 cm is not suitable because beams are not protected from damage. The results of the numerical analyses show that a satisfactory seismic performance of the innovative frames can be achieved selecting a distance of the fuse from the column flange equal to about the beam height and values of the resistance capacity ratio equal to 0.7.

7. Conclusions

This study summarizes the main results of the numerical investigations carried out on an innovative repairable fuse device for dissipative beam-to-column connections in moment-resisting composite steel frames. The device is made by introducing a discontinuity in the composite beams of a moment-resisting frame and assembling the two parts of the beam through steel plates bolted to the web and bottom flange of the beam. Two different numerical approaches are employed in this study. Detailed finite element models are used to identify the influence of some geometric and mechanical variables and to define effective configurations for the fuse device. In order to extend the results of the numerical analyses to multi-storey composite steel frames subjected to seismic excitations, simple numerical models of the device are developed and calibrated through the results of experimental tests and non-linear dynamic analyses are performed.

From an overall analysis of the numerical results, the following main conclusions can be drawn.

– Numerical investigations performed on detailed finite element models of beam-to-column sub-assemblages show that potential damage concentrates in the fuse section without any significant damage in the other structural elements. Repair work, if needed, is therefore limited to the replacement of the fuses only.

- The behavior of the fuse device is significantly affected by the geometric properties (plate thickness and cross-sectional area) and the free buckling length of the flange plate. Under hogging moment, a marked reduction of the moment capacity is registered for plates with small thickness due to buckling. An enlargement of the flange plate cross-section causes an increase of both the resistant moment and the energy dissipation capacity of the fuse. The effects of the variation of the flange plate characteristics are more evident under hogging moment and in the case of plates with small thickness.
- Innovative frames generally exhibit larger values of top displacements than conventional frames. A reduction of the base shear is registered when fuse devices are present.
- The energy dissipation capacity of innovative frames is larger than that of conventional frames. This result can be explained by the higher values of hysteretic energy dissipated by the fuses in innovative frames than by the beams in conventional frames. In general, innovative frames start dissipating energy earlier than conventional frames due to their lower stiffness and moment capacity. The plastic deformations in columns decrease slightly when fuse devices are used.
- The collapse mechanism of the innovative frames is ductile involving all the fuses and the bases of the ground level columns. The damage concentrates in fuses that can be easily replaceable. The comparison between innovative frames with fuses and conventional frames shows that the former solution is more effective to control the plastic mechanism, thus avoiding the formation of plastic deformations into the columns and minimizing the repair costs even though the initial costs of construction may be higher than those for conventional frames.
- Innovative frames with fuses exhibit larger values of the overall ductility factor than conventional frames. The high deformation capacity of the fuses was demonstrated by the results of the experimental tests.
- The importance of some geometric and mechanical characteristics of the fuse devices is highlighted in this study. The different structural response of the innovative frames depends on the moment-rotation behavior of the fuses. In particular, the effects of different values of stiffness and bending moment resistance are analyzed. In the case of low values of PGA, the smallest top displacements are generally registered for frames with fuses with high stiffness. For high values of PGA, frames with fuses with high moment resistance exhibit the smallest top displacements.
- The residual drifts of innovative frames with fuses are smaller than those of conventional frames at high ground motion intensity levels, thus allowing for an easy repair after the earthquake.
- The efficiency of the fuse device relies on proper design rules, which include the resistance capacity ratio and the location of the fuse. The location of the fuse should be chosen as a function of the resistance capacity ratio. A satisfactory seismic performance can be achieved selecting a distance of the fuse from the column flange equal to about the beam height and values of the resistance capacity ratio equal to about 0.7.

In conclusion, although the seismic performance of the examined frames can be considered comparable, economic considerations suggest that innovative frames with dissipative bolted fuses potentially result in cheaper structures when taking into account the costs of repair or replacement.

Acknowledgments

The studies reported in this paper were conducted within the scope of the FUSEIS (Dissipative Devices for Seismic Resistant Steel Frames, reference RSFR-CT-2008-00032) research project, financed by the Research Fund for Coal and Steel, of the European Commission.

References

[1] Plumier A. The dogbone: back to the future. Eng J (New York) 1997;0:61–7.
[2] Pachoumis DT, Galoussis EG, Kalfas CN, Efthimiou IZ. Cyclic performance of steel moment-resisting connections with reduced beam sections – experimental analysis and finite element model simulation. Eng Struct 2010;32:2683–92.
[3] Dubina D, Stratan A, Dinu F. Dual high-strength steel eccentrically braced frames with removable links. Earthquake Eng Struct Dynam 2008;37 (15):1703–20.
[4] Mansour N, Christopoulos C, Tremblay R. Experimental validation of replaceable shear links for eccentrically braced steel frames. J Struct Eng ASCE 2011;137(10):1141–52.
[5] Tan KG, Christopoulos C. Development of replaceable cast steel links for eccentrically braced frames. J Struct Eng ASCE 2016:1–13.
[6] Plumier A, Doneux C, Castiglioni C, Brescianini J, Crespi A, Dell'Anna S, et al. Two innovations for earthquake resistant design - the INERD project, final report. Research Programme of the Research Fund for Coal and Steel; 2004.
[7] Vayas I, Thanopoulos P. Innovative dissipative 'INERD' pin connections for seismic resistant braced frames. J Steel Struct 2005;5:453–63.
[8] Valente M. Innovative systems for seismic protection of precast industrial buildings. Appl Mech Mater 2013;274:117–20.
[9] Chan RWK, Albermani F, Williams MS. Evaluation of yielding shear panel device for passive energy dissipation. J Constr Steel Res 2009;65:260–8.
[10] Giannuzzi D, Ballarini R, Hucklebridge A, Pollino M, Valente M. Braced ductile shear panel: new seismic-resistant framing system. J Struct Eng ASCE 2014;140(2):1–11.
[11] Koetaka Y, Chusilp P, Zhang Z, Ando M, Suita K, Inoue K, et al. Mechanical property of beam-to-column moment connection with hysteretic dampers for column weak axis. Eng Struct 2005;27:109–17.
[12] Oh S-H, Kim Y-J, Ryu H-S. Seismic performance of steel structures with slit dampers. Eng Struct 2009;31:1997–2008.
[13] Balut N, Gioncu V. Suggestion for an improved 'dog-bone' solution. In: Proc conf on behaviour of steel structures in seismic areas STESSA 2003, 9-12 June 2003, Naples, Italy. p. 129–34.
[14] Shen Y, Christopoulos C, Mansour N, Tremblay R. Seismic design and performance of steel moment-resisting frames with nonlinear replaceable links. J Struct Eng ASCE 2011;137(10):1107–17.
[15] Vargas R, Bruneau M. Seismic design of multistory buildings with metallic structural fuses. In: Proceedings of the 8th U.S. national conference on earthquake engineering, April 18–22, 2006, San Francisco, California, USA. Paper No. 280.
[16] Castiglioni CA, Kanyilmaz A, Calado L. Experimental analysis of seismic resistant composite steel frames with dissipative devices. J Constr Steel Res 2012;76:1–12.
[17] Calado L, Proenca JM, Espinha M, Castiglioni CA. Hysteretic behavior of dissipative bolted fuses for earthquake resistant steel frames. J Constr Steel Res 2013;85:151–62.
[18] Calado L, Proenca JM, Espinha M, Castiglioni CA. Hysteretic behavior of dissipative welded fuses for earthquake resistant composite steel and concrete frames. Steel Compos Struct 2013;14(6):547–69.
[19] Danai D, Dougka G, Vayas I. Seismic behavior of frames with innovative energy dissipation systems (FUSEIS1-2). Eng Struct 2015;90:83–95.
[20] Simulia. ABAQUS theory manual, USA; 2007.
[21] SAP2000 static and dynamic finite element analysis of structures. Computers and Structures Inc., Berkeley, California.
[22] Vasdravellis G, Valente M, Castiglioni CA. Behavior of exterior partial-strength composite beam-to-column connections: experimental study and numerical simulations. J Constr Steel Res 2009;65(1):23–35.
[23] Vasdravellis G, Valente M, Castiglioni CA. Dynamic response of composite frames with different shear connection degree. J Constr Steel Res 2009;65(10–11):2050–61.
[24] FEMA 356. Prestandard and commentary for the seismic rehabilitation of buildings; 2000.
[25] Vanmarcke EH, Cornell CA, Gasparini DA, Hou S. SIMQKE: a program for artificial motion generation. Massachusetts: Civil Engineering Department, Massachusetts Institute of Technology; 1976.
[26] EN 1994. Eurocode 4: design of composite steel and concrete structures; 2004.
[27] EN 1998. Eurocode 8: design of structures for earthquake resistance; 2004.
[28] Braconi A, Caprili S, Degee H, Guendel M, Hjaij M, Hoffmeister B, et al. Efficiency of Eurocode 8 design rules for steel and steel-concrete composite structures. J Constr Steel Res 2015;112:108–29.
[29] ECCS Technical Committee 13. Recommended testing procedures for assessing the behaviour of structural steel elements under cyclic loads. European Convention for Constructional Steelwork (ECCS), No 45; 1986.
[30] EN 14399-2:2005. High-strength structural bolting assemblies for preloading; 2005.